

The Meta Distribution of the SINR in Joint Communication and Sensing Networks

Kun Ma, Chenyuan Feng, *Member, IEEE*, Giovanni Geraci, *Senior Member, IEEE*,
Chenxi Liu, *Senior Member, IEEE*, Meng Zhang, *Member, IEEE*, and Howard H. Yang, *Member, IEEE*

Abstract—An emerging concept in sixth-generation mobile networks is Joint Communication and Sensing (JCAS), which offers a unified approach to communication and sensing tasks. In this paper, we present a novel mathematical framework for evaluating the performance of JCAS wireless networks, utilizing stochastic geometry as an analytical tool. Our focus is on deriving the meta distribution of the signal-to-noise-plus-interference ratio (SINR) for JCAS networks. This approach provides a detailed quantification of individual user or radar performance within these networks. Our contributions include the modeling of JCAS networks and the derivation of mathematical expressions for the JCAS SINR meta distribution. Through simulations, we validate our theoretical analysis and demonstrate how the JCAS SINR meta distribution is influenced by factors such as antenna patterns, blockages, and network deployment density.

Index Terms—Joint communication and sensing, stochastic geometry, coverage probability, meta distribution, 6G.

I. INTRODUCTION

One of the envisioned features of the sixth generation (6G) mobile networks is the synergy between wireless communications and sensing [2]–[6]. Joint communication and sensing (JCAS) networks, also referred to as integrated sensing and communication (ISAC) networks, represent an emerging research topic that facilitates the effective utilization of the spectrum or waveform and paves the way for applications such as autonomous vehicles, indoor localization, urban monitoring and extended reality [7]–[9].

Recently, JCAS networks have sparked interest among researchers and industry experts due to their potential to address both communication and sensing requirements concurrently. A considerable body of prior work in this field has focused on topics such as MAC layer scheduling [10], signal processing and waveform design [11], which necessitate careful

K. Ma, M. Zhang, and H. H. Yang are with the ZJU-UIUC Institute, Zhejiang University, Haining 314400, China (e-mail: kun.22@intl.zju.edu.cn; mengzhang@intl.zju.edu.cn; haoyang@intl.zju.edu.cn).

C. Feng is with the EURECOM, Sophia Antipolis 06410, France (e-mail: Chenyuan.Feng@eurecom.fr).

G. Geraci is with Telefónica Scientific Research and Universitat Pompeu Fabra (UPF), Barcelona, Spain (e-mail: giovanni.geraci@upf.edu).

C. Liu is with the State Key Laboratory of Networking and Switching Technology, Beijing University of Posts and Telecommunications, Beijing 100876, China (email: chenxi.liu@bupt.edu.cn).

K. Ma, M. Zhang, and H. H. Yang were supported by the National Natural Science Foundation of China under Grant 62201504. G. Geraci was supported by the Spanish State Research Agency through grants CNS2023-145384, PID2021-123999OB-I00, and CEX2021-001195-M, the UPF-Fractus Chair, and by the Spanish Ministry of Economic Affairs and Digital Transformation and NextGenerationEU through the UNICO 5G I+D SORUS project.

Part of the work was presented at the IEEE 2024 International Conference on Communications Workshops (ICC Workshops) [1].

consideration of both functionalities. Therefore, it is imperative to develop tractable models and derive well-defined performance metrics to gauge the network’s effectiveness and optimize strategies that enhance both communication and sensing capabilities. In [12], the coverage and rate of JCAS networks were evaluated, along with the average performance of all user equipment (UEs) and sensed objects (SOs). The metric, however, fails to capture the performance variations across individual link. To address this concern, a fine-grained analysis is needed for JCAS network. Inspired by this, we seek to address the following question: *What fraction of UEs and SOs in the network achieve a certain link probability at predefined thresholds?* To answer this question, the meta distribution [13], which describes the entire distribution of the individual link reliability, needs to be studied. In this paper, we provide a comprehensive analysis on the signal-to-interference-and-noise (SINR) meta distribution in JCAS network.

A. Related work

Stochastic geometry has emerged as a powerful analytical framework for modeling and analyzing network-wide performance, offering theoretical models that effectively characterize various aspects of wireless communication networks. By modeling the locations of base stations (BSs) as a homogeneous Poisson point process (PPP), stochastic geometry has been successfully applied to evaluate SINR coverage probability, rate analysis, and achievable data rates in cellular networks [14], heterogeneous networks [15], and device-to-device (D2D) networks [16].

Additionally, stochastic geometry-based analysis has been extended to sensing networks. The distribution of vehicles [17]–[19] and pulsed radar sensors [20], [21] were modelled as PPPs as well. As for the performance analysis for the sensing network, different performance metrics are adopted for radar detection and parameter estimation models. For instance, [18] examines the radar detection range and false alarm rate in relation to the radar detection scenario by taking the strongest interferer approximation into account. By characterizing the cumulative distribution of the signal-to-clutter-and-noise-ratio (SCNR) as the detection coverage probability, [22] quantified the radar detection performance with a focus on discrete clutter conditions. Such a metric simplifies computation compared to traditional metrics such as detection probability and false alarm rates, while still providing substantial insights. Regarding the parameter estimation problem, [12] associates the classic metric Cramer-Rao lower bound (CRLB) with

SINR, demonstrating the utility of stochastic geometry in such problems. In summary, stochastic geometry significantly contributes to sensing applications by providing models to characterize the system's SINR or SCNR.

In recent years, stochastic geometry has surfaced as a strong analytical framework for JCAS networks. For instance, time-sharing networks were explored in [20], detailing their radar detection range, false alarm rates, and communication success probabilities. In [23], a joint radar communication system was studied, in which BS performs downlink communication towards mobile users after successfully detecting them using the integrated radar. The concepts of coverage probability and ergodic capacity were extended to the radar applications in [12], where the upper and lower bounds of these metrics were calculated for communication and sensing, respectively. Additionally, [24] derived the ergodic rate and coverage probability of sensing and communication in a coexistence network, considering the coupling effects of these two functions and formulating the joint performance of the overall network. Other studies, such as [25] and [26], focused on the energy and spectrum efficiency, formulating optimization problem with respect to BS deployment to maximize the network performance.

Despite these advancements, there remains a knowledge vacuum regarding the unique behavior of users or radar systems in a JCAS network. Most existing studies have primarily concentrated on the coverage probability, a geographic average that only provides information about the expected JCAS performance across all network deployments, thus overlooking the variability in user or radar experiences. For instance, two network realizations may exhibit the same spatial average, but one may display a wider range of success probabilities (for instance, from 0.5 to 0.99), while the other may display a narrower range (for instance, from 0.85 to 0.95). This indicates the need for a more granular performance analysis tool.

The concept of the meta distribution, introduced in [13], addresses this need by characterizing the cumulative distribution function (CCDF) of the conditional success probability (CSP), treating it as a random variable dependent on the point process realization. This metric allows the quantification of the proportion of links that achieve a given SINR threshold and exceed the required reliability level. As a result, the meta distribution has been widely applied in communication networks [16], [27], [28] and sensing networks [19], [29]. Specifically, [19] computed the meta distribution for a vehicle detection scenario and assessed the average local radar detection latency. In [29], the meta distribution of the SCNR was used to calculate the variance in detection coverage, providing insights into the reliability of detection performance. As previous work has been confined to either communication or radar detection, our work fills the gap by deriving meta distribution for JCAS networks.

B. Contributions

To fill in the research gap, we investigate the SINR meta distribution in the JCAS network in this research. We perform a comprehensive investigation on the performance of the

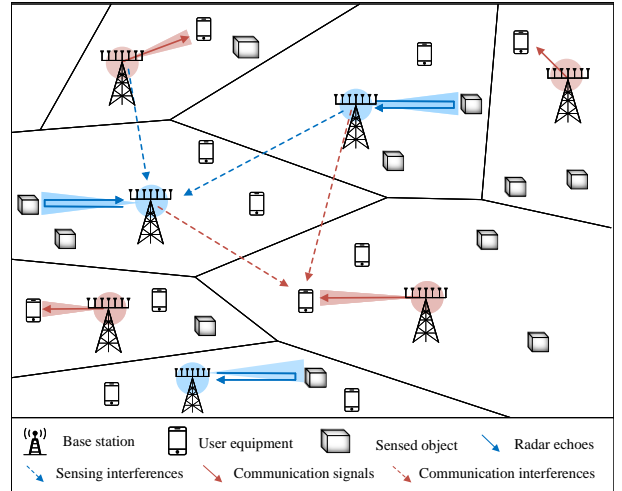


Fig. 1: Illustration of the JCAS network considered, with BSs simultaneously sending information packets to UEs and sensing waveforms to the SOs for which they receive radar echoes.

network under reasonable assumptions. The contribution of this paper are summarized as follows:

- We establish an analytical framework for modeling the JCAS network. Our analysis is tractable and incorporates key features including path loss, small-scale fading, antenna patterns, network blockage, and random network topology.
- We derive the analytical expressions of the moments of the conditional success probability for both communication and sensing, respectively, which are then used to obtain the SINR meta distribution of the JCAS network. We further explore the asymptotic behavior of the UE/SO densities and present several relevant special cases to potentially simplify the analytical results.
- Our analysis is validated through extensive simulations. Numerical results are provided to demonstrate how the JCAS SIR meta distribution responds to different network deployment configurations. The results demonstrate that increasing the proportion of UEs in the network and enhancing the antenna directivity at the BSs could improve the JCAS performance. Furthermore, the results also reveal that incorporating blockage and increasing BS densities will enhance the sensing performance, while there is no such monotonicity for communication performance.

The rest of the paper is organized as follows: Section II presents the system model. Section III provides the analytical results. Section IV provides the numerical results and analysis. Finally, the entire work is concluded by Section V.

II. SYSTEM MODEL

A. Network Deployment

We consider a JCAS wireless network, comprising several base stations (BSs), user equipment (UEs), and sensed objects (SOs), as depicted in Fig. 1. The locations of the BSs, UEs, and SOs are modeled as three independent homogeneous Poisson

point processes (PPPs), denoted by Φ_b , Φ_u , and Φ_s , with intensities of λ_b , λ_u , and λ_s , respectively. The BSs are in charge of sending information packets to UEs in the downlink or sending sensing waveforms to the SOs and receiving echoes from them. Communication and sensing functionalities are performed using a shared multicarrier waveform that is reused throughout the network, leading to interference among transmissions from different nodes. We assume that each BS is active and selects one randomly assigned entity (either a UE or SO) within its coverage area to provide the appropriate service. It is also assumed that $\lambda_u \gg \lambda_b$ and $\lambda_s \gg \lambda_b$, meaning each cell will contain multiple UEs and SOs. Furthermore, each wireless transmission channel is subject to Rayleigh fading and path loss, which follows a power-law distribution, with the BSs transmitting at a given power P_{tx} .

B. Propagation Model and Association Policies

First, we characterize the large-scale path loss in the propagation model. Depending on whether a blockage intersects the link, a pair of transmitters and receivers can have a line-of-sight (LoS) or non-line-of-sight (NLoS) link. We use the blockage probability model from [30], where the probability of establishing an LoS link with a length r is given by

$$p_L(r) = \exp(-\beta r), \quad (1)$$

and the probability of establishing a NLoS link is

$$p_N(r) = 1 - p_L(r), \quad (2)$$

where β is a parameter capturing the density of blockages.

Note that communications can occur over either an LoS or NLoS link, each characterized by distinct system factors. Specifically, the path loss function for a link of length r is given by

$$L(r) = \begin{cases} K_L r^{-\alpha_L}, & \text{w.p. } p_L(r), \\ K_N r^{-\alpha_N}, & \text{w.p. } 1 - p_L(r), \end{cases} \quad (3)$$

where K_L and K_N denote the channel gains associated with LoS and NLoS links, respectively, and α_L and α_N are path loss exponents for LoS and NLoS links, respectively.

The association of UEs to BSs and the selection of BSs for SO measurement play an important role in coverage and rate. Specifically, we assume that each UE is connected to the BS with the smallest path loss, via either LoS or NLoS links. Moreover, we consider a monostatic sensing scenario in which the BSs transmit sensing waveforms and receive echoes from the SOs. We assume only the SOs with LoS links are viable for wireless sensing, as detecting or estimating the location of a NLoS object is particularly challenging in practice. Consequently, each SO is associated with the nearest BS with an LoS path.

C. Antenna Pattern

We consider that all BSs and UEs perform directional beamforming for both communication and sensing purposes. For analytical tractability, we utilize a sector model [31] to model the antenna pattern of BSs and UEs. Specifically, we model the radar as having a single omnidirectional element transmitter

and a receiver equipped with a uniform planar square antenna array and half-wavelength antenna spacing between antennas. The main 3 dB beamwidth, main lobe gain, and front-to-back ratio (ratio of sidelobe gain to main lobe gain) of the antenna are denoted as ψ , G , and ξ , respectively. Moreover, we assume the BS is equipped with a full-duplex transceiver to facilitate monostatic sensing [32]. In what follows, we use the subscripts b, u, t, and r to refer to the antenna patterns of the BS, UE, transmitter, and receiver, respectively.

For a communication link, the BS and UE select the direction of the main lobe to maximize the received power. For a sensing link, since sensing only occurs over an LoS link, the BS directs both its transmit and receive beams toward the desired SO. Perfect alignment is assumed between the typical UE/SO and its serving BS. Consequently, the gain for the desired signal at the typical UE is $G_{b,t}G_{u,r}$, while the gain for the radar return is $G_{b,t}G_{b,r}$.

For interfering links that are not aligned with the intended receiver, we model their antenna gains as independent random variables. More precisely, the normalized antenna gain between the transmitting BS and receiving UE over the k -th interfering link is given by

$$\bar{G}_{b,t}^k = \begin{cases} 1, & \text{w.p. } p_{b,t} = \frac{\psi_{b,t}}{2\pi}, \\ \xi_{b,t}, & \text{w.p. } 1 - p_{b,t}, \end{cases} \quad (4)$$

and

$$\bar{G}_{u,r}^k = \begin{cases} 1, & \text{w.p. } p_{u,r} = \frac{\psi_{u,r}}{2\pi}, \\ \xi_{u,r}, & \text{w.p. } 1 - p_{u,r}. \end{cases} \quad (5)$$

According to the SO association policy, the serving BS always directs its beams toward the desired SO. However, interference arises from other BSs as well as from the serving BS itself, rather than from the SO. Consequently, the interference pattern in the sensing scenario is non-isotropic. As outlined in [12], the normalized antenna gain of the receiving BS can be expressed as

$$\bar{G}_{b,r}^k(r_0, r_k) = \begin{cases} 1, & \text{w.p. } p_{b,r}(r_0, r_k), \\ \xi_{u,t}, & \text{w.p. } 1 - p_{b,r}(r_0, r_k), \end{cases} \quad (6)$$

in which

$$p_{b,r}(r_0, r_k) = \frac{\frac{\psi_{b,r}}{2} - J(r_k; r_0, \max\{\cos(\frac{\psi_{b,r}}{2}), \frac{r_k}{2r_0}\}) \mathbb{1}\{r_k \leq 2r_0\}}{\pi - J(r_k; r_0, \frac{r_k}{2r_0}) \mathbb{1}\{r_k \leq 2r_0\}}, \quad (7)$$

and function $J(r; r_0, z)$ is given by

$$J(r; r_0, z) = \int_z^1 (1 - u^2)^{-\frac{1}{2}} \exp\left(-\beta \sqrt{r^2 - 2rr_0u + r_0^2}\right) du, \quad (8)$$

where r_0 and r_k represent the distances from the serving BS and the k -th interfering BS to the typical SO, respectively.

To this end, the normalized antenna gains for the communication and sensing links of the k -th interfering node, denoted by $g_c^k = \bar{G}_{b,t}^k \bar{G}_{u,r}^k$ and $g_s^k = \bar{G}_{b,t}^k \bar{G}_{b,r}^k$, respectively, are discrete random variables evaluated at $a_{c,j}$ and $a_{s,j}$ ($j \in \{1, 2, 3, 4\}$) with probability $p_{c,j}$ and $p_{s,j}(r_0, r_k)$, as shown in Table I.

TABLE I: Different Evaluations and Probabilities of $G_{c,i}$ and $G_{s,i}$

j	1	2	3	4
$a_{c,j}$	1	$\xi_{b,t}$	$\xi_{u,r}$	$\xi_{b,t}\xi_{u,r}$
$p_{c,j}$	$p_{b,t}p_{u,r}$	$(1-p_{b,t})p_{u,r}$	$p_{b,t}(1-p_{u,r})$	$(1-p_{b,t})(1-p_{u,r})$
$a_{s,j}$	1	$\xi_{b,t}$	$\xi_{b,r}$	$\xi_{b,t}\xi_{b,r}$
$p_{s,j}$	$p_{b,t}p_{b,r}$	$(1-p_{b,t})p_{b,r}$	$p_{b,t}(1-p_{b,r})$	$(1-p_{b,t})(1-p_{b,r})$

D. SINR Models

Based on Slivnyark's theorem [33], we focus on a typical UE situated at the origin. This typical UE is connected to the BS via either LoS or NLoS links with minimal path loss. Let X_0 denote the location of the tagged BS (also referred to as the *typical BS*) of the *typical UE* and X_k denote the location of the k -th BS in the network. The normalized noise power at the receiver is defined as

$$\bar{\sigma}_c^2 = \frac{\sigma^2}{G_{b,t}G_{u,r}P_{tx}}, \quad (9)$$

where σ^2 denotes the noise power. Then, the SINR received at the typical UE can be expressed as

$$\text{SINR}_c = \frac{h_0 L(\|X_0\|)}{\sum_{k \neq 0} h_k g_c^k L(\|X_k\|) + \bar{\sigma}_c^2}, \quad (10)$$

where $h_k \sim \exp(1)$ is the channel fading from the k -th BS to the typical UE, g_c^k represents the total normalized effective antenna gain of the k -th interfering link, and $\|\cdot\|$ denotes the Euclidean norm.

Similarly, in a monostatic sensing scenario where the BSs transmit the sensing waveforms and listen to the echo of the SOs, without loss of generality, we place the *typical SO* at the origin [12]. According to [34], the signal strength of the radar echo measured at the typical BS is given by

$$\begin{aligned} S_s &= \frac{P_{tx} G_{b,t} G_{b,r} \lambda_w^2 \sigma_{cs} L_{ret}(\|X_0\|)}{(4\pi)^3} \\ &= A \frac{\sigma_{cs}}{4\pi} L_{ret}(\|X_0\|), \end{aligned} \quad (11)$$

where $G_{b,t}$ and $G_{b,r}$ denote the antenna gains of transmission and reception in the sensing stage, respectively, λ_w is the carrier wavelength, $\sigma_{cs} \sim \exp(1)$ represents the radar cross-section, which can be modeled as a random variable that follows the exponential distribution with unit mean [35], and $A = P_{tx} G_{b,t} G_{b,r} (\lambda_w/4\pi)^2$.

Since sensing utilizes the same carrier as communication, the interference accumulated at the typical BS can be expressed as

$$I_s = \sum_{k \neq 0} A \tilde{h}_k g_s^k L(\|X_k - X_0\|), \quad (12)$$

where $\tilde{h}_k \sim \exp(1)$ stands for the channel fading from the k -th BS to the typical BS, g_s^k denotes the normalized effective antenna gain from the k -th interfering link. As a simplification, we assume the LoS/NLoS status of the interfering BSs with

respect to the typical BS is independent of the LoS/NLoS status of the BSs observed by the typical SO. Let the normalized noise power at the typical BS for typical SO be defined as

$$\bar{\sigma}_s^2 = \frac{\sigma^2}{G_{b,t} G_{b,r} P_{tx}}. \quad (13)$$

By analogy with the communication scenario, the sensing SINR at the typical BS can be written as follows

$$\begin{aligned} \text{SINR}_s &= \mathbb{1}\{\|X_0\| < \infty\} \frac{S_s}{I_s} \\ &= \mathbb{1}\{\|X_0\| < \infty\} \frac{\frac{\sigma_{cs}}{4\pi} L_{ret}(\|X_0\|)}{\sum_{k \neq 0} \tilde{h}_k g_s^k L(\|X_k - X_0\|) + \bar{\sigma}_s^2}, \end{aligned} \quad (14)$$

where $\mathbb{1}\{\|X_0\| < \infty\}$ indicates that sensing link is LoS path only, and thus, SINR is zero if there are no LoS links between the BSs and the typical SO.

We note that while SINR_c is an actual SINR, SINR_s is a conceptual one, constructed as a proxy for the BS's efficacy in estimating the SO's parameter of interest.¹ Based on these SINR models, we can establish suitable metrics to assess the JCAS network performance.

E. Performance Metric

The probability that SINR_c surpasses a decoding threshold θ_c is known as the coverage probability or success probability, a widely-used metric to evaluate link performance in cellular networks. This metric provides information about the fraction of UEs in the network that achieves an SINR at least equal to θ_c . A similar definition can be applied to sensing performance. The estimation rate, defined as the mutual information between the radar return and the parameter of interest divided by the coherent processing interval, characterizes the quality of sensing, with upper and lower bounds determined by logarithmic functions of SINR_s [12]. Hence, sensing accuracy can be captured using a measure based on the distribution of SINR_s . For instance, one could consider the sensing coverage probability, which is defined as the probability that SINR_s exceeds a predetermined threshold θ_s and reflects the average portion of the SOs whose SINR meets or exceeds θ_s .

Since coverage probabilities provide only average JCAS performance across all network deployments, this paper employs the concept of conditional coverage probability (a.k.a. conditional transmission success probability) and the meta SINR distribution [13], [27], [28] to obtain a fine-grained perspective of the JCAS network performance. Specifically, given the PPP Φ_b , we define the *conditional JCAS coverage probability* as the joint fraction of UEs or SOs whose corresponding SINR exceeds their corresponding threshold, given by

$$\begin{aligned} P(\theta_c, \theta_s) &= \mathbb{P}_{\Phi_u + \Phi_s}(\text{SINR} > \theta_c \mid \Phi_b) \\ &\stackrel{(a)}{=} \frac{\lambda_u}{\lambda_u + \lambda_s} P_c(\theta_c) + \frac{\lambda_s}{\lambda_u + \lambda_s} P_s(\theta_s), \end{aligned} \quad (15)$$

where

$$P_c(\theta_c) = \mathbb{P}_{\Phi_u}(\text{SINR}_c > \theta_c \mid \Phi_b), \quad (16)$$

¹In the following, for the sake of readability, we neglect the constant multiplier $\frac{1}{4\pi}$ in (14) as it can be embedded into the decoding threshold.

and

$$P_s(\theta_s) = \mathbb{P}_{\Phi_s}(\text{SINR}_s > \theta_s \mid \Phi_b) \quad (17)$$

stands for the conditional communication and sensing coverage probabilities, respectively, and (a) follows from the independence of Φ_u and Φ_s and using the superposition theorem for the stationary process. (15) indicates that by conditioning on the BS topology, the strongly coupled relationship of communication and sensing due to co-existence of BS deployments can be eliminated. Hence we can analyze the performance of communication and sensing separately when characterizing the JCAS network.

We note that $P(\theta_c, \theta_s)$ remains a random variable because, although channel fading is averaged out, the randomness stemming from Φ_b persists². In that respect, we leverage the concept of the SINR meta distribution in communication networks [13] and define the *JCAS SINR meta distribution* as the complementary cumulative distribution function (CCDF) of $P(\theta_c, \theta_s)$, i.e.,

$$F(\theta_c, \theta_s, x) = \mathbb{P}(P(\theta_c, \theta_s) > x). \quad (18)$$

This quantity provides information about the fraction of end terminals (UEs or SOs) in the network that can attain the desired SINR (at levels of θ_c and θ_s for SINR_c and SINR_s , respectively) with a reliability (i.e., probability) of at least x .

III. ANALYSIS OF JCAS SINR META DISTRIBUTION

This section details the steps to derive analytical expressions for the quantity in (18). First, we calculate the general moments of the conditional sensing and communication coverage probabilities. Then, we derive the analytical expression for the JCAS SINR meta distribution.

A. Moments of Conditional Sensing Coverage Probability

We begin by deriving the conditional sensing coverage probability $P_s(\theta_s)$ by averaging out the randomness introduced by channel fading. The quantity $P_s(\theta_s)$ represents the probability that, given a network realization Φ_b , the effect of channel fading results in sensing SINR_s exceeding the threshold θ_s .

Lemma 1. *Conditioned on the point process Φ_b , the sensing coverage probability is given by*

$$P_s(\theta_s) = \prod_{i \in \{L, N\}} \prod_{X_k \in \Phi_{b \setminus X_0}^i} \left(\sum_{j=1}^4 \frac{p_{s,j}(\|X_0\|, \|X_k - X_0\|)}{1 + \frac{\theta_s K_i a_{s,j} \|X_0\|^{\alpha_L}}{K_L \|X_k - X_0\|^{\alpha_i}}} \right) \times \exp\left(-\frac{\theta_s \bar{\sigma}_s^2}{K_L} \|X_0\|^{2\alpha_L}\right) \left(1 - \exp\left(\frac{-2\pi\lambda_b}{\beta^2}\right)\right), \quad (19)$$

where $\Phi_{b \setminus X_0}^L$ and $\Phi_{b \setminus X_0}^N$ represent the interfering nodes in Φ_b with LoS and NLoS paths to the serving BS, respectively.

²The conventional coverage probability can be obtained by taking the expectation of $P(\theta_c, \theta_s)$ with respect to Φ_b , thereby disregarding the dependence of the JCAS performance on the network realization Φ_b .

Proof: Using (14), we can calculate the conditional JCAS coverage probability as

$$\begin{aligned} P(\theta_s) &= \mathbb{P}_{\Phi_s}(\text{SINR}_s > \theta_s \mid \Phi_b) \\ &\stackrel{(a)}{=} \mathbb{P}\left(\sigma_{cs} > \frac{\theta_s \sum_{k \neq 0} \tilde{h}_k g_s^k L(\|X_k - X_0\|) + \theta_s \bar{\sigma}_s^2}{L_{\text{ret}}(\|X_0\|)} \mid \|X_0\| < \infty, \Phi_b\right) \times \mathbb{P}(\|X_0\| < \infty) \\ &\stackrel{(b)}{=} \mathbb{E}\left[\exp\left(-\theta_s \sum_{k \neq 0} \tilde{h}_k g_s^k \frac{L(\|X_k - X_0\|)}{L_{\text{ret}}(\|X_0\|)}\right) \mid \|X_0\| < \infty\right] \\ &\quad \times \exp\left(-\frac{\theta_s \bar{\sigma}_s^2}{K_L} \|X_0\|^{2\alpha_L}\right) \left(1 - \exp\left(\frac{-2\pi\lambda_b}{\beta^2}\right)\right) \\ &\stackrel{(c)}{=} \prod_{i \in \{L, N\}} \prod_{X_k \in \Phi_{b \setminus X_0}^i} \left(\frac{1}{1 + \theta_s g_s^k \frac{K_i \|X_0\|^{\alpha_L}}{K_L \|X_k - X_0\|^{\alpha_i}}}\right) \\ &\quad \times \exp\left(-\frac{\theta_s \bar{\sigma}_s^2}{K_L} \|X_0\|^{2\alpha_L}\right) \left(1 - \exp\left(\frac{-2\pi\lambda_b}{\beta^2}\right)\right) \\ &\stackrel{(d)}{=} \prod_{i \in \{L, N\}} \prod_{X_k \in \Phi_{b \setminus X_0}^i} \left(\sum_{j=1}^4 \frac{p_{s,j}(\|X_0\|, \|X_k - X_0\|)}{1 + \theta_s a_{s,j} \frac{K_i \|X_0\|^{\alpha_L}}{K_L \|X_k - X_0\|^{\alpha_i}}}\right) \\ &\quad \times \exp\left(-\frac{\theta_s \bar{\sigma}_s^2}{K_L} \|X_0\|^{2\alpha_L}\right) \left(1 - \exp\left(\frac{-2\pi\lambda_b}{\beta^2}\right)\right), \quad (20) \end{aligned}$$

where (a) follows from that $P(\|X_0\| < \infty) = 1 - \exp\left(\frac{-2\pi\lambda_b}{\beta^2}\right)$ [36], (b) follows from the fact that σ_{cs} obeys an exponential distribution, (c) holds because fading realizations are also exponentially distributed and mutually independent, as well as the independence of point processes $\Phi_{b \setminus X_0}^L$ and $\Phi_{b \setminus X_0}^N$, while (d) follows from the independence of g_s^k . \square

Using the above results, we can derive different moments of $P(\theta_s)$, which are presented below.

Theorem 1. *The b -th moment of the conditional sensing coverage probability is given by*

$$\begin{aligned} M_b^s &= \left(1 - \exp\left(\frac{-2\pi\lambda_b}{\beta^2}\right)\right)^{b-1} \int_0^\infty f(r_0) \exp\left(-\frac{b\theta_s \bar{\sigma}_s^2}{K_L} r_0^{2\alpha_L}\right) \\ &\quad - \sum_{i \in \{L, N\}} \int_0^\infty \left(1 - \left(\sum_{j=1}^4 \frac{p_{s,j}(r, r_0)}{1 + \theta_s a_{s,j} \frac{K_i r_0^{2\alpha_L}}{K_L r^{\alpha_i}}}\right)^b\right) \lambda_i(r, r_0) dr \Big) dr_0, \quad (21) \end{aligned}$$

in which

$$f(r_0) = 2\pi\lambda_b r_0 p_L(r_0) \exp\left(\frac{-2\pi\lambda_b}{\beta^2} (1 - e^{-\beta r_0} (\beta r_0 + 1))\right), \quad (22)$$

and

$$\lambda_i(r, r_0) = 2p_i(r) \lambda_b r \left(\pi - J(r; r_0, \frac{r}{2r_0}) \mathbb{1}\{r \leq 2r_0\}\right). \quad (23)$$

Proof: Please refer to Appendix A. \square

Notably, the first moment of the conditional sensing coverage probability is the standard sensing SINR coverage probability of the network, denoted as M_1^s , which is given by

$$\begin{aligned} M_1^s &= \int_0^\infty f(r_0) \exp\left(-\frac{\theta_s \bar{\sigma}_s^2}{K_L} r_0^{2\alpha_L} - \sum_{i \in \{L, N\}} \right. \\ &\quad \left. \int_0^\infty \left(1 - \sum_{j=1}^4 \frac{p_{s,j}(r, r_0)}{1 + \theta_s a_{s,j} \frac{K_i r_0^{2\alpha_L}}{K_L r^{\alpha_i}}}\right) \lambda_i(r, r_0) dr\right) dr_0. \quad (24) \end{aligned}$$

B. Moments of Conditional Communication Coverage Probability

Similar to the previous section, we commence our analysis by deriving an initial expression for the conditional communication coverage probability.

Lemma 2. *Given typical UE is associated with a BS through either LoS or NLoS paths, the conditional communication coverage probability is*

$$P_{c,\rho}(\theta_c) = \prod_{i \in \{L,N\}} \prod_{X_k \in \Phi_i} \left(\sum_{j=1}^4 \frac{p_{c,j}}{1 + \frac{\theta_c b_{c,j}^k K_i \|X_0\|^{\alpha_\rho}}{K_\rho \|X_k\|^{\alpha_i}}} \right) \times \exp\left(-\frac{\theta_c \bar{\sigma}_c^2}{K_\rho} \|X_0\|^{\alpha_\rho}\right), \quad \rho \in \{L, N\}, \quad (25)$$

where ρ indicates whether the path between the serving BS and the typical UE is LoS or NLoS, Φ_L and Φ_N are the interfering BSs whose communication links toward the typical UE is LoS and NLoS, respectively.

Proof: This can be proven using a method similar to that of Lemma 1, and is therefore omitted here. \square

Since communication can occur over either LoS or NLoS links, the conditional communication coverage probability can be obtained by averaging out the randomness in the link status, i.e.

$$P_c(\theta_c) = A_L P_{c,L} + A_N P_{c,N}, \quad (26)$$

where A_L and A_N denote the probabilities that the typical UE establishes a LoS and NLoS to its associated BS, respectively, as given by [36]

$$A_L = B_L \int_0^\infty e^{-\pi \lambda_b \int_0^{\phi_{L,N}(x)} (1-p_L(t)) t dt} f(x) dx, \quad (27)$$

where $f(x)$ is defined in (22), B_L and $\phi_{\rho,i}(r_0)$, $\rho, i \in \{L, N\}$ are given by the following, respectively,

$$B_L = 1 - e^{2\pi \lambda_b \int_0^\infty r p_L(r) dr}, \quad (28)$$

$$\phi_{\rho,i}(r_0) = (K_i/K_\rho)^{1/\alpha_i} r_0^{\alpha_\rho/\alpha_i}, \quad (29)$$

and $A_N = 1 - A_L$.

Next, we can derive the expressions for various moments of $P_c(\theta_c)$.

Theorem 2. *The b -th moment of the conditional communication coverage probability is given by*

$$M_b^c = \sum_{\rho \in \{L,N\}} \int_0^\infty \hat{f}_\rho(r_0) \exp\left(-\frac{b\theta_c \bar{\sigma}_c^2}{K_\rho} r_0^{\alpha_\rho} - 2\pi \lambda_b \sum_{i \in \{L,N\}} \int_{\phi_{\rho,i}(r_0)}^\infty \left(1 - \left(\sum_{j=1}^4 \frac{p_{c,j}}{1 + \theta_s a_{c,j} \frac{K_i}{K_\rho} r_0^{\alpha_\rho} r^{-\alpha_i}}\right)^b\right) r p_i(r) dr\right) dr_0, \quad (30)$$

where

$$\hat{f}_L(r_0) = 2\pi \lambda_b r_0 p_L(r_0) \exp\left(-2\pi \lambda_b \left(-\frac{e^{-\beta r_0}(\beta r_0 + 1)}{\beta^2} + \frac{\phi_{L,N}^2(r_0)}{2} + \frac{e^{-\beta \phi_{L,N}(r_0)}(\beta \phi_{L,N}(r_0) + 1)}{\beta^2}\right)\right), \quad (31)$$

and

$$\hat{f}_N(r_0) = 2\pi \lambda_b r_0 p_N(r_0) \exp\left(-2\pi \lambda_b \left(\frac{r_0^2}{2} + \frac{e^{-\beta r_0}(\beta r_0 + 1)}{\beta^2} - \frac{e^{-\beta \phi_{N,L}(r_0)}(\beta \phi_{N,L}(r_0) + 1)}{\beta^2}\right)\right). \quad (32)$$

Proof: According to [36, Lemma 3], given that the typical UE is associated with a LoS/NLoS BS, the probability density function (pdf) of the distance to its serving BS (denoted by r_0) is

$$f_\rho(r_0) = \hat{f}_\rho(r_0)/A_\rho, \quad \rho \in \{L, N\}, \quad (33)$$

where $\hat{f}_L(r_0)$ and $\hat{f}_N(r_0)$ are defined in (31) and (32), respectively. Then, the result may be proven similarly to Theorem 1 by calculating the moments conditioned on r_0 and then subsequently de-conditioning using (33). \square

We also provide the standard communication coverage probability in the following corollary.

Corollary 1. *Given that the typical UE is associated with a LoS BS, the first moment of conditional communication coverage probability (a.k.a. the standard communication SINR coverage probability) is given as*

$$M_1^{c,L} = \int_0^\infty f_L(r_0) \exp\left(-\frac{\theta_c \bar{\sigma}_c^2}{K_L} r_0^{\alpha_L} - \lambda_b (A_L(r_0) - A_N(r_0) + B(r_0))\right) dr_0, \quad (34)$$

where

$$A_i(r_0) = \frac{(\beta r_0 + 1)e^{-\beta r_0}}{\beta^2} \left(\sum_{j=1}^4 \frac{p_{c,j}}{1 + \theta_{i,j} r_0^{-\alpha_i}} - 1 \right) + \frac{\alpha_i}{\beta^2} \sum_{j=1}^4 \bar{\theta}_{i,j} p_{c,j} \sum_{n=0}^\infty \frac{1}{\beta^{-\alpha_i(n+1)}} \left(e^{-\beta r_0} (\beta r_0)^{n-\alpha_i} + (1 - \alpha_i(n+1)) \Gamma(1 - \alpha_i(n+1), \beta r_0) \right), \quad (35)$$

and

$$B(r_0) = \frac{1}{2} \sum_{j=1}^4 \bar{\theta}_{N,j} p_{c,j} {}_2F_1(2, -\delta_N - 1; 1 - \delta_N; -\bar{\theta}_{N,j} r_0^{\alpha_N}) + \frac{r_0^2}{2} \left(\sum_{j=1}^4 \frac{p_{c,j}}{1 + \bar{\theta}_{N,j} r_0^{-\alpha_N}} - 1 \right), \quad (36)$$

whereas $\bar{\theta}_{i,j} = \theta_s a_{c,j} K_i r_0^{\alpha_L} / K_L$, $\delta_N = 2/\alpha_N$, $\Gamma(s, x) = \int_x^\infty t^{s-1} e^{-t} dt$ represents Gamma incomplete function.

Proof: Please refer to Appendix B. \square

The coverage probability given the typical UE is associated with a NLoS BS can also be obtained by substituting $f_L(r_0)$ and $\theta_s a_{c,j} K_i r_0^{\alpha_L} / K_L$ with $f_N(r_0)$ and $\theta_s a_{c,j} K_i r_0^{\alpha_N} / K_N$ in (34).

C. JCAS SINR Meta Distribution

Finally, using the moments of both the conditional communication coverage probability and the conditional sensing coverage probability, we derive the JCAS SINR meta distribution, defined as the CCDF of $P(\theta_c, \theta_s)$.

Theorem 3. *The meta distribution of the SINR in the JCAS network under consideration is given by*

$$F(\theta_c, \theta_s, x) = \frac{1}{2} + \frac{1}{\pi} \int_0^\infty \text{Im} \left\{ x^{-j\omega} M_{j\omega}^{\text{JCAS}} \right\} \frac{d\omega}{\omega}, \quad (37)$$

where $\text{Im}\{\cdot\}$ denotes the imaginary part of the input variable, $j = \sqrt{-1}$, and M_b is the b -th moment of $P(\theta_c, \theta_s)$, given by

$$M_b^{\text{JCAS}} = \frac{1}{(\lambda_u + \lambda_s)^b} \sum_{m=0}^{\infty} \binom{b}{m} \lambda_u^{b-m} \lambda_s^m M_{b-m}^c M_m^s. \quad (38)$$

where M_{b-m}^c is the $(b-m)$ -th moment of $P_c(\theta_c)$ and M_m^s is the m -th moment of $P_s(\theta_s)$.

Proof: The b -th moment of $P(\theta_c, \theta_s)$ can be calculated as

$$\begin{aligned} M_b^{\text{JCAS}} &= \mathbb{E} \left\{ P(\theta_c, \theta_s)^b \right\} \\ &\stackrel{(a)}{=} \frac{1}{(\lambda_u + \lambda_s)^b} \mathbb{E} \left\{ \sum_{m=0}^{\infty} \binom{b}{m} \lambda_u^{b-m} P_c(\theta_c)^{b-m} \lambda_s^m P_s(\theta_s)^m \right\} \\ &\stackrel{(b)}{=} \frac{1}{(\lambda_u + \lambda_s)^b} \sum_{m=0}^{\infty} \binom{b}{m} \lambda_u^{b-m} \mathbb{E}[P_c(\theta_c)^{b-m}] \lambda_s^m \mathbb{E}[P_s(\theta_s)^m] \\ &= \frac{1}{(\lambda_u + \lambda_s)^b} \sum_{m=0}^{\infty} \binom{b}{m} \lambda_u^{b-m} \lambda_s^m M_{b-m}^c M_m^s, \end{aligned} \quad (39)$$

where (a) follows from the binomial expansion and (b) follows from the independence of $P_c(\theta_c)$ and $P_s(\theta_s)$. The proof is completed by invoking the Gil-Paleaz theorem [37]. \square

As a byproduct, we can obtain the JCAS coverage probability by computing the first moment of (39) with respect to Φ_b , given by:

$$M_1^{\text{JCAS}} = \frac{\lambda_u M_1^c + \lambda_s M_1^s}{\lambda_u + \lambda_s}, \quad (40)$$

which is consistent with the definition in [12]. Such a metric reflects the joint fraction of UEs and SOs whose coverage conditions are satisfied.

Moreover, when $\lambda_s \gg \lambda_u$, the network is considered to be sensing only. The meta-distribution for such a network can be derived using the Gil-Paleaz theorem, given by

$$F(\theta_s, x) = \frac{1}{2} + \frac{1}{\pi} \int_0^\infty \text{Im} \left\{ x^{-j\omega} M_{j\omega}^s \right\} \frac{d\omega}{\omega}. \quad (41)$$

Similarly, when $\lambda_u \gg \lambda_s$, the meta distribution of communication SINR is given by

$$F(\theta_c, x) = \frac{1}{2} + \frac{1}{\pi} \int_0^\infty \text{Im} \left\{ x^{-j\omega} M_{j\omega}^c \right\} \frac{d\omega}{\omega}. \quad (42)$$

D. Approximation of the JCAS SINR Meta Distribution

According to Theorem 3, the derivation of meta distribution requires calculating the moments of the coverage probability of communication, M_b^c , and sensing, M_b^s . However, calculating M_b^s involves tedious numerical calculations of nested integrations due to the intricate interfering BSs process and its antenna pattern. It is notable that the probability of the normalized antenna gain of the receiving BS taking a value of 1, $p_{b,r}$, as defined in (7), is lower bounded by $\frac{\psi_{b,r}}{2}$. Therefore,

we can use this lower bound to accelerate the computation, with its accuracy validated in Fig. 3.

While Theorem 3 provides an exact analytical expression for the JCAS SINR meta distribution, evaluating it can be computationally expensive due to the infinite summation and the calculation of imaginary moments in (39). Since the value of the conditional JCAS coverage probability ranges from 0 to 1, we simplify the expression by approximating the conditional JCAS coverage probability in (19) using a beta distribution [13]. This approximation is achieved by matching the first and second moments, M_1 and M_2 . The former is provided in (40), and the latter can be readily obtained from (39), given by:

$$M_2^{\text{JCAS}} = \frac{\lambda_u^2 M_2^c + 2\lambda_u \lambda_s M_1^c M_1^s + \lambda_s^2 M_2^s}{(\lambda_u + \lambda_s)^2}. \quad (43)$$

Thus, the meta distribution of the SINR in the JCAS network in (37) can then be approximated as

$$F(\theta_c, \theta_s, x) \approx 1 - I_v \left(\frac{\beta \mu}{1 - \mu}, \beta \right), \quad v \in [0, 1], \quad (44)$$

where $I_v(x, y) = \int_0^{1-v} z^{x-1} (1-z)^{y-1} dz / B(x, y)$ is the regularized incomplete beta function, with $B(\cdot, \cdot)$ denoting the beta function. Here, $\mu = M_1$ and $\beta = \frac{(M_1 - M_2)(1 - M_1)}{M_2 - M_1^2}$.

E. Special Cases

Although Theorem 1 and Theorem 2 provide general results for the moments of conditional sensing and communication coverage probabilities in a complex form, simpler and more intuitive expressions can be derived under specific link conditions or deployment scenarios. We now turn our attention to several relevant special cases.

1) Sensing and Communication on Orthogonal Channel

In the system model under consideration, communication and sensing functions are executed using a shared multicarrier waveform, which results in interference among transmissions from different nodes. Here, we examine a scenario where communication and sensing are allocated on orthogonal time-frequency resources.

When communication and sensing tasks are conducted on separate frequency bands, interference for each task arises only from BSs concurrently performing the same task, rather than from all BSs as previously discussed.

Corollary 2. *If communication and sensing are allocated orthogonal frequency-time resource units in the JCAS network, the b -th moment of the conditional sensing coverage probability and that of the conditional communication coverage probability are, respectively, given by*

$$\begin{aligned} M_b^s &= \left(1 - \exp \left(-\frac{2\pi \lambda_b}{\beta^2} \right) \right)^{b-1} \int_0^\infty f(r_0) \exp \left(-\frac{b\theta_s \bar{\sigma}_s^2}{K_L} r_0^{2\alpha_L} - \right. \\ &\left. \delta_s \sum_{i \in \{L, N\}} \int_0^\infty \left(1 - \left(\sum_{j=1}^4 \frac{p_{s,j}(r, r_0)}{1 + \theta_s a_{s,j} \frac{K_i r_0^{2\alpha_L}}{K_L r^{\alpha_i}}} \right)^b \right) \lambda_i(r, r_0) dr \right) dr_0, \end{aligned} \quad (45)$$

and

$$M_b^c = \sum_{\rho \in \{L, N\}} \int_0^\infty \hat{f}_\rho(r_0) \exp\left(-\frac{b\theta_c \bar{\sigma}_c^2}{K_\rho} r_0^{\alpha_\rho} - 2\pi\delta_c \lambda_b \sum_{i \in \{L, N\}} \int_{\phi_{\rho, i}(r_0)}^\infty \left(1 - \left(\sum_{j=1}^4 \frac{p_{c, j}}{1 + \theta_s a_{c, j} \frac{K_i r_0^{\alpha_\rho}}{K_\rho r^{\alpha_i}}}\right)^b\right) r p_i(r) dr\right) dr_0. \quad (46)$$

where δ_s and $\delta_c = 1 - \delta_s$ denote the proportion of interfering BSs that simultaneously perform sensing/communication tasks.

Proof: Since each BS supports communication and sensing but only on separate frequency bands, the distance of a typical UE/SO to its serving BS r_0 follows the same distribution $f(r_0)$ or $\hat{f}_\rho(r_0)$ as in Theorem 1 and Theorem 2. For a given sensing link, the interfering BSs transmitting on the same frequency are a thinned version of the original PPP and have a density $k\lambda_b$. Since a thinned version of a PPP is a PPP, the rest of the proof follows Theorem 1 and Theorem 2. \square

Note that under a random scheduling policy [38], where during each downlink time slot each BS randomly chooses to perform sensing or communication with a certain probability, the proportion coefficients in Corollary 2 are determined by said probability.

2) Noise-Limited Case

Due to the large bandwidth in the mmWave frequency band, mmWave networks can be considered noise-limited when BSs are sparsely deployed [39]. In this scenario, the b -th moment of conditional sensing coverage probability can be significantly simplified.

Corollary 3. *If the JCAS network is noise limited, the b -th moment of conditional sensing coverage probability is given by*

$$M_b^s = \left(1 - \exp\left(\frac{-2\pi\lambda_b}{\beta^2}\right)\right)^{b-1} \int_0^\infty f(r_0) \times \exp\left(-\frac{b\theta_s \bar{\sigma}_s^2}{K_L} r_0^{2\alpha_L}\right) dr_0, \quad (47)$$

and conditional communication coverage probability is given by

$$M_b^c = \sum_{\rho \in \{L, N\}} \int_0^\infty \hat{f}_\rho(r_0) \exp\left(-\frac{b\theta_c \bar{\sigma}_c^2}{K_\rho} r_0^{\alpha_\rho}\right) dr_0. \quad (48)$$

Proof: This can be easily proven by taking the expectations of σ_{CS} , h_0 and r_0 , respectively. \square

3) Asymptotic Antenna Behaviour

For mmWave networks, it is both crucial and interesting to explore how performance varies with the size of the BS antenna array. For simplicity, we assume that the number of the antenna elements at both the BS transmitter and receiver is the same, denoted as N_b . According to [40], the relationship between the antenna parameters and the size of the antenna array is given by:

$$\psi = \frac{\sqrt{3}}{\sqrt{N_b}}, \quad (49)$$

$$G = N_b, \quad (50)$$

$$\xi = \frac{1}{N_b \sin^2\left(\frac{3\pi}{2\sqrt{N_b}}\right)}. \quad (51)$$

We examine two specific cases of the antenna pattern for BSs, one where $N_b = 1$, corresponding to an omnidirectional antenna array, and the other where $N_b \rightarrow \infty$, corresponding to an extremely massive antenna array.

When $N_b = 1$, we have $\xi = 1$, indicating that the antenna has the same radiation pattern in all directions. The moment of the conditional sensing coverage probability is then given by:

$$M_b^s = \left(1 - \exp\left(\frac{-2\pi\lambda_b}{\beta^2}\right)\right)^{b-1} \int_0^\infty f(r_0) \exp\left(-\frac{b\theta_s \bar{\sigma}_s^2}{K_L} r_0^{2\alpha_L}\right) - \sum_{i \in \{L, N\}} \int_{r_0}^\infty \left(1 - \left(\frac{1}{1 + \theta_s \frac{K_i r_0^{2\alpha_L}}{K_L r^{\alpha_i}}}\right)^b\right) 2\pi r p_i(r) dr\right) dr_0. \quad (52)$$

On the other hand, the beamforming effect for communication still exists because the antenna arrays of UE remain unchanged. Therefore, when $N_a = 1$, the moment of the conditional communication coverage probability is given by:

$$M_b^c = \sum_{\rho \in \{L, N\}} \int_0^\infty \hat{f}_\rho(r_0) \exp\left(-\frac{b\theta_c \bar{\sigma}_c^2}{K_\rho} r_0^{\alpha_\rho} - 2\pi\lambda_b \sum_{i \in \{L, N\}} \int_{\phi_{\rho, i}(r_0)}^\infty \left(1 - \left(\frac{p_{u, r}}{1 + \theta_s \frac{K_i r_0^{\alpha_\rho}}{K_\rho r^{\alpha_i}}} + \frac{1 - p_{u, r}}{1 + \theta_s \xi_{u, r} \frac{K_i r_0^{\alpha_\rho}}{K_\rho r^{\alpha_i}}}\right)^b\right) \times r p_i(r) dr\right) dr_0. \quad (53)$$

When extremely large antenna arrays are used, i.e., as $N_b \rightarrow \infty$, the expression for the moment of the conditional sensing coverage probability is given by the following corollary.

Corollary 4. *When $N_b \rightarrow \infty$, the b -th moment of the conditional sensing coverage probability and that of the conditional communication coverage probability are, respectively, given by*

$$\lim_{N_b \rightarrow \infty} M_b^s = \left(1 - \exp\left(\frac{-2\pi\lambda_b}{\beta^2}\right)\right)^{b-1} \int_0^\infty f(r_0) \exp\left(-\sum_{i \in \{L, N\}} \int_0^\infty \left(1 - \left(\frac{1}{1 + \left(\frac{4}{9\pi^2}\right) \frac{\theta_s K_i r_0^{2\alpha_L}}{K_L r^{\alpha_i}}}\right)^b\right) \lambda_i(r, r_0) dr\right) dr_0, \quad (54)$$

and

$$\lim_{N_b \rightarrow \infty} M_b^c = \sum_{\rho \in \{L, N\}} \int_0^\infty \hat{f}_\rho(r_0) \exp\left(-2\pi\lambda_b \sum_{i \in \{L, N\}} \int_{\phi_{\rho, i}(r_0)}^\infty \left(1 - \left(\frac{p_{u, r}}{1 + \frac{4\theta_s K_i r_0^{\alpha_\rho}}{9\pi^2 K_\rho r^{\alpha_i}}} + \frac{1 - p_{u, r}}{1 + \frac{4\theta_s \xi_{u, r} K_i r_0^{\alpha_\rho}}{9\pi^2 K_\rho r^{\alpha_i}}}\right)^b\right) \times r p_i(r) dr\right) dr_0. \quad (55)$$

Proof: From the expression for the main lobe gain G in (50) and the normalized noise power $\bar{\sigma}_s^2$ in (13), when $N_b \rightarrow \infty$, we have $\bar{\sigma}_s^2 \rightarrow 0$, indicating that the noise effect can be neglected. Similarly, algebraic operations yield $\psi \rightarrow 0$, $p_{b, r}(r_0, r_k) \rightarrow 0$ and $\xi \rightarrow \frac{4}{9\pi^2}$ when $N_b \rightarrow \infty$. Substituting these limit results into (46), we can obtain the final result. \square

This corollary provides the following sights: (1) As $N_b \rightarrow \infty$, the effect of noise is completely suppressed, as the normalized noise powers $\bar{\sigma}_s^2 \rightarrow 0, \bar{\sigma}_c^2 \rightarrow 0$, making the network interference-limited. (2) For a sensing link, as $N_b \rightarrow \infty$, the normalized total antenna gain of interfering links approaches an isotropic value with a constant gain of $\frac{4}{9\pi^2}$.

4) No Blockage and Isotropic antennas

To gain further insights, we consider a special case where the blockage parameters are sufficiently small and the BSs are equipped with isotropic antennas instead.

Corollary 5. *Ignoring the blockage effects in the network and assuming constant antenna gains, i.e. $\beta \rightarrow 0$, $G_s = G_c = 1$, the b -th moment of $P(\theta_s)$ can be simplified as*

$$M_b^s = \int_0^\infty 2\pi\lambda_b r_0 \exp(-\lambda_b(\pi r_0^2 + F_b^s(r_0)) - \frac{b\theta_s \bar{\sigma}_s^2}{K_L} r_0^{2\alpha_L}) dr_0, \quad (56)$$

with

$$\begin{aligned} F_b^s(r_0) = & 4\pi r_0^2 \left({}_2F_1(b, \delta_L; 1 + \delta_L; \theta_s (\frac{r_0}{2})^{\frac{2}{\delta_L}} - 1) \right. \\ & + 4r_0^2 \sum_{n=0}^{\infty} \frac{\Gamma(n + \frac{1}{2})}{\Gamma(\frac{1}{2})n!(1+2n)} C\left(b, \theta_s (\frac{r_0}{2})^{\frac{2}{\delta_L}}, \delta_L(n + \frac{3}{2})\right) \\ & \left. + 2\pi r_0^2 C\left(b, \theta_s (\frac{r_0}{2})^{\frac{2}{\delta_L}}, \delta_L\right), \right) \end{aligned} \quad (57)$$

where $\delta_L = 2/\alpha_L$, $\Gamma(\cdot)$ is the gamma function, whilst

$$C(x, y, z) = 1 - {}_2F_1\left(x, x+z; x+z+1; -\frac{1}{y}\right) \times \frac{z}{y^x(x+z)}, \quad (58)$$

and the conditional communication coverage probability is

$$M_b^c = \frac{1}{{}_2F_1(b, -\delta_L; 1 - \delta_L; -\theta_c)}. \quad (59)$$

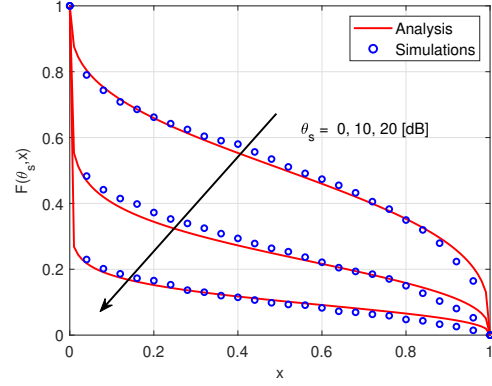
Proof: Please refer to Appendix C. \square

IV. NUMERICAL RESULTS

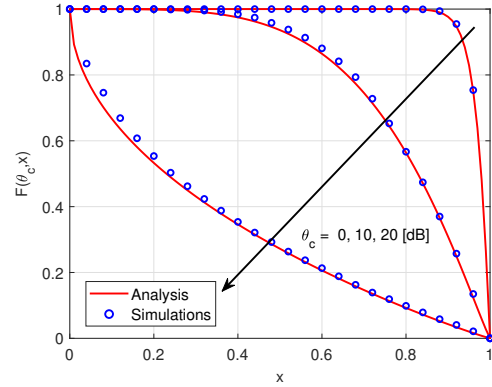
This section presents the numerical results to validate our analysis and evaluate how the JCAS SINR meta distribution is influenced by the SINR thresholds and by the BS density.

A. Experiment Setup

We generate 1000 PPP realizations for the locations of BSs, UEs, and SOs. Within each Voronoi cell formed by the BSs, UEs and SOs are distributed in a square area measuring 1,000 meters on each side. Once the topology is constructed, it remains unchanged, but the fading realizations of communications and sensing across each link are recalculated over 1,000 time periods. We then collect statistics for communications and sensing to compute the conditional JCAS coverage probability for each realization. Unless otherwise specified, we use the following parameters path loss exponent and channel gains associated with LoS and NLoS links: $\alpha_L = 2.5$, $\alpha_N = 4$, $K_L = -75.96$ dB, $K_N = -90.96$ dB. We set densities for BSs, UEs and SOs to $\lambda_b = 10^{-4} \text{ m}^{-2}$, and $\lambda_u = \lambda_s = 10^{-3} \text{ m}^{-2}$. The blockage density is set to $\beta = 0.0071$, which corresponds to an urban environment [12]. The power and antenna parameters are $P_{tx} = 15$ dB, $\sigma^2 = -100$ dB, the number of antenna elements at the BS transceiver is $N_b = 64$, corresponding to a highly directional antenna array [16], and the number of antenna elements at the UE receiver is $N_u = 16$.



(a) Meta distribution of sensing SINR for $\theta_s = 0, 10, 20$ dB.



(b) Meta distribution of communication SINR for $\theta_c = 0, 10, 20$ dB.

Fig. 2: SINR meta distribution given in Theorem 1 and Theorem 2, and simulations, as a function of the reliability threshold (x -axis) and for different SINR thresholds (θ_c, θ_s).

B. Performance Comparison & Analysis

Fig. 2 plots the simulated CCDF of the conditional sensing and communication coverage probability (black circles) with the analytical results from Theorem 1 and Theorem 2 across various pairs of communication and sensing thresholds. The JCAS SINR meta distribution in Fig. 2 provides a fine-grained evaluation of the network performance in terms of both communication and sensing. For instance, Fig. 2 (a) shows that for $\theta_s = 0$ dB and 20 dB, respectively, setting a reliability threshold of 0.6 on the x -axis corresponds to values of approximately 0.47 and 0.08 on the y -axis, respectively. This indicates that 47% of the SOs in this network can achieve sensing SINRs of at least 0 dB with a 60% reliability. However, this fraction decreases to 8% when both SINR thresholds are raised to 20 dB.

Fig. 3 compares the meta distribution of conditional sensing coverage probability with its approximation. It is observed that the gap between the approximation and the exact results diminishes as BS density increases, verifying that the approximation serves as a tight lower bound to the exact results across various BS densities. This occurs because the lower bound primarily introduces error in the interference component, which becomes less significant in a regime of low BS density.

Fig. 4 plots the JCAS SINR meta distribution in Theorem 3

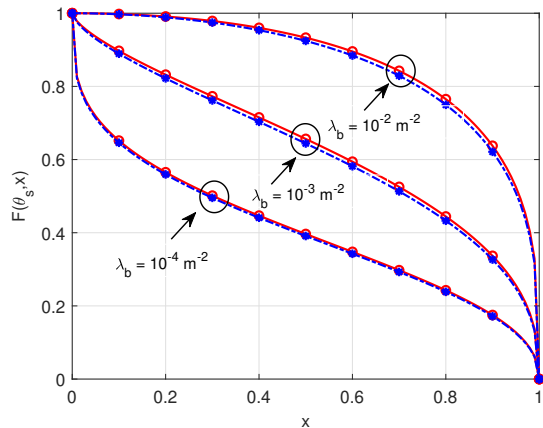


Fig. 3: Distribution of the conditional sensing coverage probability in Section and the approximation

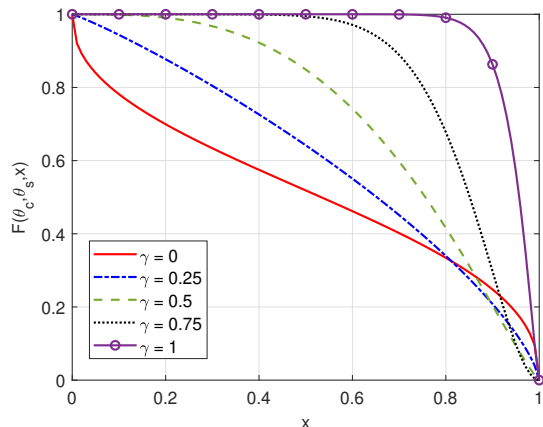


Fig. 4: JCAS SINR meta distribution as a function of the reliability threshold under different UE density ratio γ , where $\gamma \triangleq \lambda_u/(\lambda_u + \lambda_s)$, and the SINR thresholds are set as $\theta_c = \theta_s = 0$ dB.

across various UEs and SOs densities. We observe that, for the same SINR detection threshold $\theta_c = \theta_s$, scenarios with a higher UE density ratio $\gamma = \lambda_u/(\lambda_u + \lambda_s)$ exhibit a higher JCAS SINR coverage probability. This is because, unlike communication, sensing experiences double path loss and only occurs under LoS conditions. Consequently, increasing the proportions of scheduled communication transmissions with respect to sensing transmissions results in a higher coverage probability. It is notable that for high reliability thresholds, the meta distribution of sensing coverage may exceed that of communication. This anomalous behavior occurs when the serving BS is unrealistically close to the typical UE/SO, resulting in higher signal strength for sensing under the given power law path loss model.

Fig. 5 presents a comparison of the meta distribution for both communication and sensing under different time-frequency resource allocation strategies. The meta distribution for the case where communication and sensing operate on orthogonal frequency bands is derived using Corollary 2, with the proportion coefficients set to $\delta_c = 0.7$ and $\delta_s = 0.3$

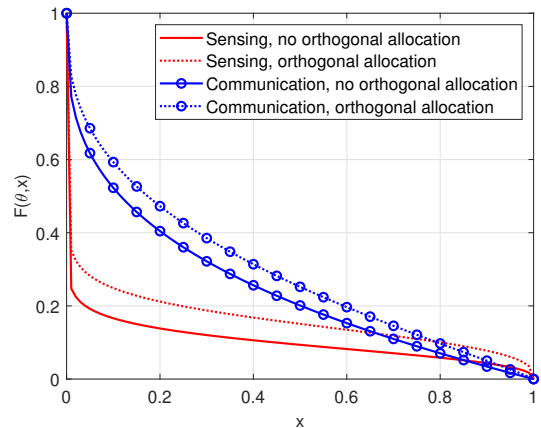


Fig. 5: The SINR meta distribution as a function of the reliability threshold for both communication and sensing under different allocation policies.

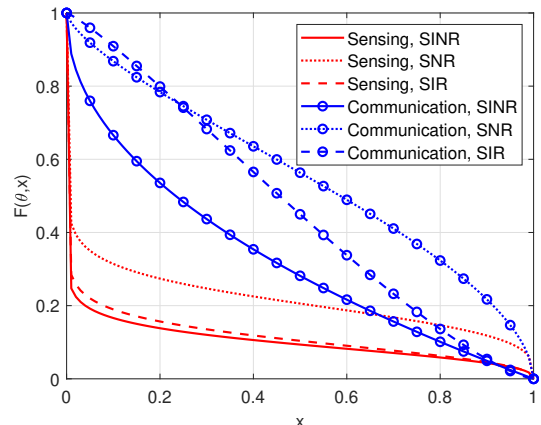
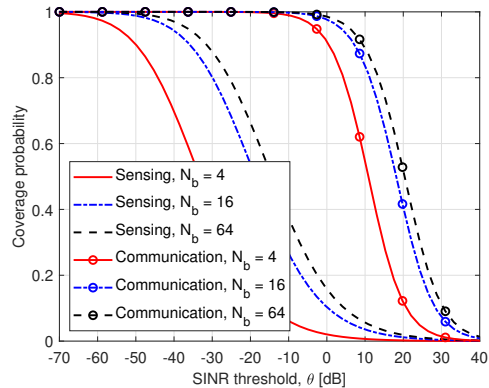


Fig. 6: The SINR, SIR, and SNR meta distribution as a function of the reliability threshold for both communication and sensing.

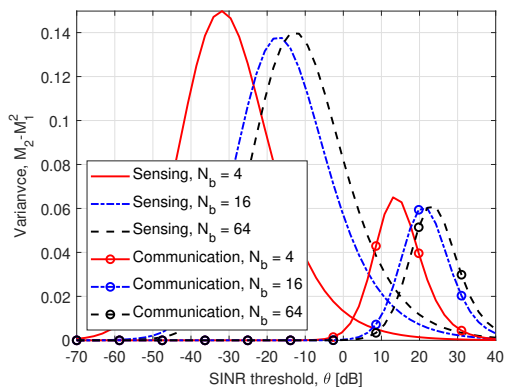
[38]. As illustrated in the figure, orthogonal allocation can enhance the performance of both communication and sensing by mitigating interference.

In Fig. 6, we compare the meta distribution of the SINR, SIR and SNR for both communication and sensing, assuming a noise power is set as $\sigma^2 = -100$ dB. Here, the meta distribution of SNR is obtained by Corollary 3, while the SIR meta distribution is obtained by setting the normalized noise power as $v_c = v_s = 0$. The close alignment between the SIR and SINR curves in sensing indicates that interference plays a more significant role in determining link quality for sensing, whereas both noise and interference are equivalently non-negligible for communication. This disparity is partly due to the fact that interference BSs experience greater path loss relative to the typical SO than the serving BS, yet interference accumulates at the serving BS. Consequently, the path loss between the interference BSs and the serving BS may exceed that of the desired path.

Fig. 7 (a) presents the analytical results for the standard coverage probability across different BS antenna array sizes,



(a) The coverage probability.



(b) The variance of conditional coverage probability

Fig. 7: The impact of antenna array size on the mean and variance of conditional coverage probability for both communication and sensing.

N_b , for both communication and sensing. As shown in this figure, increasing the number of BS antennas improves the standard coverage probability. This is expected, as a larger antenna array forms narrower beams, leading to reduced interference, while the increased main lobe gain decreases normalized noise power. Another observation is that communication coverage probability is more sensitive to changes in the SINR threshold, suggesting that sensing performance exhibits greater variability across SOs compared to communication performance across UEs. Fig. 7 (b) illustrates the variance of the conditional coverage probability as a function of decoding thresholds, under varying antenna array sizes. Notably, as the variance approaches zero at the extremes of θ , i.e., $\theta \rightarrow 0$ or $\theta \rightarrow \infty$, it reaches a maximum at a finite value θ^* . It is observed that θ^* increases with N_a , though the variance does not follow a strictly monotonic relationship with antenna size. This figure indicates that network variance peaks differently as antenna size changes, implying that performance fluctuations in wireless links are directly influenced by the size of the antenna array.

Fig. 8 depicts the communication and sensing coverage probabilities as a function of BS deployment density, under varying levels of blockage. We consider a low-blockage regime ($\beta = 0.0028$), where the median LoS probability occurs at 50 meters, and a moderate-blockage regime ($\beta = 0.0071$),

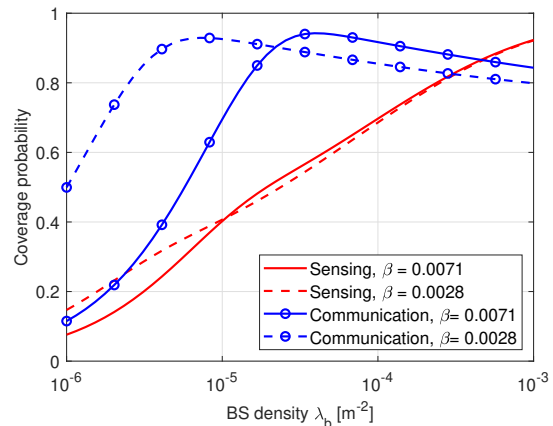


Fig. 8: Coverage probabilities of communication and sensing versus BS density λ_b under different blockage parameters.

corresponding to an urban environment. Consistent with the findings in [12], our result demonstrates that for a fixed blockage parameter, the sensing coverage probability increases with BS deployment density. In contrast, communication coverage probability peaks at a certain value of λ_b and then declines. This discrepancy arises due to the additional factor of two in the path loss exponent for sensing signals. When viewing increasing BS density as a reduction in the distance of all links, the marginal improvement in desired signal power for sensing outstrips that of interference power, owing to the double path loss exponent. For communication, however, interference have larger increment in the high BS density regime, leading to a degradation of the performance. Another notable observation is that both communication and sensing coverage probability increases with the blockage parameter β at high BS densities and decreases at low densities. This can be attributed to the fact that increasing blockage reduces both interference and desired signal power, and wireless links are dominated by interference in high or moderate BS density regimes, and by desired signal strength in low-density regimes.

V. CONCLUSION

In this paper, we developed an analytical framework for evaluating the performance of JCAS in wireless networks by employing stochastic geometry as a key tool. Our approach involved deriving mathematical expressions for the conditional JCAS coverage probability and its distribution, known as the SINR meta distribution, which offers much sharper results than traditional SINR coverage performance obtained through spatial averaging. Our theoretical models, validated by simulations, effectively capture the impact of network deployment density on JCAS SINR performance. The numerical results reveal several noteworthy insights: Under the assumptions we made for antenna pattern, blockage and association policy, 1) Equipping BSs with large antenna arrays is anticipated to optimize JCAS performance; 2) Network densification improve sensing performance, although no such monotonic relationship exists for communication performance. Our work have made assumptions for tractability and one extension would be generalizing the simplified rayleigh fadin

model to more general Nakagami fading model [36], adopting a more realistic antenna model and taking the shadow effect into account. Future research directions include incorporating a minimum inter-site distance between BSs and exploring temporal dynamics, such as data traffic for communication [41] and status updates for sensing [42].

APPENDIX A: PROOF OF THEOREM 1

The b -th moment of $P_s(\theta_s)$ can be expressed as:

$$M_b^s = \mathbb{E}_{r_0} \left\{ \underbrace{\left\{ \prod_{i \in \{L, N\}} \prod_{X_k \in \Phi_{b \setminus X_0}^i} \left(\frac{1}{1 + \frac{\theta_s K_i \|X_0\|^{\alpha_L}}{K_L \|X_k - X_0\|^{\alpha_i}}} \right) \right\}}_{F_{b|r_0}} \right\} \times \left(-\frac{b\theta_s v_s}{K_L} \|X_0\|^{2\alpha_L} \right) \|X_0\| \left(1 - \exp\left(-\frac{2\pi\lambda_b}{\beta^2}\right) \right)^b. \quad (60)$$

Then, one must determine the moment of conditional coverage probability of sensing conditioned on the distance between the serving BS and the origin, $r_0 = \|X_0\|$.

Lemma 2 of [12] states that the point process of the distance of interfering BSs with regard to serving BS conditioned on r_0 is a PPP on \mathbb{R}_+ with the following intensity function, provided as $\Pi_b^0 = \{\|X_k - X_0\| : X_k \in \Phi_b^{X_0}\}$:

$$\lambda_b^0(r; r_0) = 2\lambda_b r \left(\pi - J(r, r_0) \mathbb{1}\{r \leq 2r_0\} \right), \quad (61)$$

where $J(r, r_0)$ is defined as in (8).

Applying independent thinning theorem to Π_b^0 with respect to the LoS/NLoS status, the intensity function of interfering BSs Π_b^0 can be divided into two independent processes

$$\lambda_i(r; r_0) = p_i(t) \lambda_b^0(r, r_0), \quad i \in \{L, N\}. \quad (62)$$

Then via the probability generating functional (PGFL) of PPP, $F_{b|r_0}$ can be derived as

$$F_{b|r_0} = \exp \left(- \sum_{i \in \{L, N\}} \int_0^\infty \left(1 - \frac{1}{(1 + \theta_s \frac{K_i}{K_L} r_0^{2\alpha_L} r^{-\alpha_i})^b} \right) \times \lambda_i^0(r; r_0) dr \right). \quad (63)$$

Given the typical user observes at least one LoS base station, the conditional probability density function of its distance to the nearest LOS base station is given by [36, Lemma 1]:

$$f_L(x) = \frac{2\pi\lambda_b x p_L(x) \exp\left(-\frac{2\pi\lambda_b}{\beta^2}(1 - e^{-\beta x}(\beta x + 1))\right)}{1 - \exp(-2\pi\lambda_b/\beta^2)}. \quad (64)$$

Then, substituting (63) into (60) and de-conditioning on r_0 using (64), we obtain the b -th moment in (21).

APPENDIX B: PROOF OF COROLLARY 1

The standard coverage probability can be obtained by assigning b as 1 :

$$M_1^{C,L} = \int_0^\infty f_L(r_0) \exp \left(-\frac{\theta_c \bar{\sigma}_c^2}{K_L} r_0^{\alpha_L} - \lambda_b (A_L(r_0) - A_N(r_0) + B(r_0)) \right) dr_0, \quad (65)$$

where

$$A_i = \int_{r_0}^\infty \left(1 - \sum_{j=1}^4 \frac{p_{c,j}}{1 + \theta_s a_{c,j} \frac{K_i r_0^{\alpha_L}}{K_L r^{\alpha_i}}} \right) 2\pi r \exp(-\beta r) dr, \quad (66)$$

$$B = \int_{r_0}^\infty \left(1 - \sum_{j=1}^4 \frac{p_{c,j}}{1 + \theta_s a_{c,j} \frac{K_N r_0^{2\alpha_L}}{K_L r^{\alpha_N}}} \right) 2\pi r dr. \quad (67)$$

For A_i , using the integration by parts, we have

$$\begin{aligned} A_i &= \frac{(\beta r_0 + 1)e^{-\beta r_0}}{\beta^2} \left(\sum_{j=1}^4 \frac{p_{c,j}}{1 + \bar{\theta}_{i,j} r_0^{-\alpha_i}} - 1 \right) \\ &\quad + \int_{r_0}^\infty \sum_{j=1}^4 \bar{\theta}_{i,j} \alpha_i p_{c,j} \frac{r^{-\alpha_i-1}}{(1 + \bar{\theta}_{i,j} r^{-\alpha_i})^2} \frac{(\beta r + 1)e^{-\beta r} dr}{\beta^2} \\ &\stackrel{(a)}{=} \frac{(\beta r_0 + 1)e^{-\beta r_0}}{\beta^2} \left(\sum_{j=1}^4 \frac{p_{c,j}}{1 + \bar{\theta}_{i,j} r_0^{-\alpha_i}} - 1 \right) \\ &\quad + \frac{\alpha_i}{\beta^2} \sum_{j=1}^4 \bar{\theta}_{i,j} p_{c,j} \sum_{n=0}^\infty \frac{1}{\beta^{-\alpha_i}(n+1)} \left(e^{-\beta r_0} (\beta r_0)^{n-\alpha_i} \right. \\ &\quad \left. + (-\alpha_i(n+1) + 1) \Gamma(-\alpha_i(n+1) + 1, \beta r_0) \right), \quad (68) \end{aligned}$$

where (a) uses Taylor expansion of $(1 + \bar{\theta}_{i,j} r^{-\alpha_i})^{-2}$, and $\bar{\theta}_{i,j} = \theta_s a_{c,j} K_i r_0^{\alpha_L} / K_L$, $\delta_N = 2/\alpha_N$. On the other hand, by algebraic operations, B can be calculated as

$$\begin{aligned} B &= \frac{1}{2} \sum_{j=1}^4 \bar{\theta}_{N,j} p_{c,j} {}_2F_1(2, -\delta_N - 1; 1 - \delta_N; -\bar{\theta}_{N,j} r_0^{\alpha_N}) \\ &\quad + \frac{r_0^2}{2} \left(\sum_{j=1}^4 \frac{p_{c,j}}{1 + \bar{\theta}_{N,j} r_0^{-\alpha_N}} - 1 \right), \quad (69) \end{aligned}$$

where ${}_2F_1(\cdot, \cdot; \cdot, \cdot)$ is the Gaussian hyper-geometric function.

APPENDIX C: PROOF OF COROLLARY 5

The derivation of moment of conditional communication success probability has been given in [13], and thus we provide the proof of sensing case. Conditioned on the distance from the typical SO and serving BS, when the NLOS BSs is ignored, the intensity measure of Π_b^0 may be simplified into

$$\lambda_b^0(r; r_0) = 2\lambda_b r \left(\pi - \arccos\left(\frac{r}{2r_0}\right) \mathbb{1}\{r \leq 2r_0\} \right). \quad (70)$$

Then $F_{b|r_0}$ in (60) can be simplified into

$$\begin{aligned} M_{b|r_0}^s &= \exp \left(- \int_{\mathbb{R}^2} \left[1 - \frac{1}{(1 + \theta_s r_0^{2\alpha_L} r^{-\alpha_L})^b} \right] \lambda_b^0(r; r_0) dr \right) \\ &\stackrel{(a)}{=} \exp \left(- 4\lambda_b \pi r_0^2 \delta_L \int_0^1 \left(1 - \frac{1}{(1 + \theta_s (\frac{r_0}{2})^{\frac{2}{\delta_L}} v)^b} \right) v^{-\delta_L-1} dv \right. \\ &\quad \left. - 2\lambda_b \pi r_0^2 \delta_L \int_1^\infty \left(1 - \frac{1}{(1 + \theta_s (\frac{r_0}{2})^{\frac{2}{\delta_L}} v)^b} \right) v^{-\delta_L-1} dv \right. \\ &\quad \left. - 4\lambda_b r_0^2 \delta_L \sum_{n=0}^\infty \frac{\Gamma(n + \frac{1}{2})}{\Gamma(\frac{1}{2}) n! (1 + 2n)} \right. \\ &\quad \left. \times \int_1^\infty \left(1 - \frac{1}{(1 + \theta_s (\frac{r_0}{2})^{\frac{2}{\delta_L}} v)^b} \right) v^{-\delta_L(n+\frac{3}{2})-1} dv \right) \\ &\stackrel{(b)}{=} \exp(-\lambda_b F_b^s(r_0)), \quad (71) \end{aligned}$$

where step (a) follows by the substitution of $v = (\frac{2r_0}{r})^{\alpha_L}$ and the Taylor expansion of $\arcsin(x)$, step (b) follows by the algebraic operation and $F_b^s(r_0)$ is defined as (57).

Since blockage effect is neglected, the typical SO is now associated with the nearest base station. Then the pdf of the distance between the serving BS and the typical BS r_0 distance follows a Rayleigh distribution as $f_R(r_0) = 2\pi\lambda_b r_0 e^{-\lambda_b \pi r_0^2}$. The proof is concluded by de-conditioning on r_0 .

REFERENCES

- [1] K. Ma, C. Feng, G. Geraci, and H. H. Yang, "The meta distribution of the SIR in joint communication and sensing networks," in *IEEE Int. Conf. Commun. Workshops (ICC Workshops)*, June 2024, pp. 1–6.
- [2] D. Lopez-Perez, N. Piovesan, and G. Geraci, "Capacity and power consumption of multi-layer 6G networks using the upper mid-band," *arXiv preprint arXiv: 2411.09660*, 2024.
- [3] F. Tariq, M. R. Khandaker, K.-K. Wong, M. A. Imran, M. Bennis, and M. Debbah, "A speculative study on 6G," *IEEE Wireless Commun.*, vol. 27, no. 4, pp. 118–125, Aug. 2020.
- [4] E. Oughton, G. Geraci, M. Polese, V. Shah, D. Buble, and S. Blue, "Reviewing wireless broadband technologies in the peak smartphone era: 6G versus Wi-Fi 7 and 8," *Telecommunications Policy*, vol. 48, no. 6, p. 102766, 2024.
- [5] S. Dang, O. Amin, B. Shihada, and M.-S. Alouini, "What should 6G be?" *Nature Electronics*, vol. 3, no. 1, pp. 20–29, 2020.
- [6] S. Guo and K. Qu, "Unified integrated sensing and communication signal design: A sphere packing perspective," *IEEE Trans. Commun.*, pp. 1–1, 2024.
- [7] F. Liu, C. Masouros, A. P. Petropulu, H. Griffiths, and L. Hanzo, "Joint radar and communication design: Applications, state-of-the-art, and the road ahead," *IEEE Trans. Commun.*, vol. 68, no. 6, pp. 3834–3862, 2020.
- [8] J. A. Zhang, M. L. Rahman, K. Wu, X. Huang, Y. J. Guo, S. Chen, and J. Yuan, "Enabling joint communication and radar sensing in mobile networks—A survey," *IEEE Commun. Surv. Tutor.*, vol. 24, no. 1, pp. 306–345, 2021.
- [9] D. Cong, S. Guo, S. Dang, and H. Zhang, "Vehicular behavior-aware beamforming design for integrated sensing and communication systems," *IEEE Trans. Intell. Transp. Syst.*, vol. 24, no. 6, pp. 5923–5935, 2023.
- [10] H. Li, "Mac scheduling in joint communications and sensing networks based on virtual queues," in *IEEE Global Commun. Conf. (GLOBECOM)*, 2022, pp. 4069–4074.
- [11] P. Kumari, J. Choi, N. González-Prelcic, and R. W. Heath, "Ieee 802.11 ad-based radar: An approach to joint vehicular communication-radar system," *IEEE Trans. Veh. Technol.*, vol. 67, no. 4, pp. 3012–3027, 2017.
- [12] N. R. Olson, J. G. Andrews, and R. W. Heath Jr, "Coverage and capacity of joint communication and sensing in wireless networks," *arXiv preprint arXiv: 2210.02289*, 2022.
- [13] M. Haenggi, "The meta distribution of the SIR in Poisson bipolar and cellular networks," *IEEE Trans. Wireless Commun.*, vol. 15, no. 4, pp. 2577–2589, Apr. 2016.
- [14] J. G. Andrews, F. Baccelli, and R. K. Ganti, "A tractable approach to coverage and rate in cellular networks," *IEEE Trans. Commun.*, vol. 59, no. 11, pp. 3122–3134, Nov. 2011.
- [15] H. S. Dhillon, R. K. Ganti, F. Baccelli, and J. G. Andrews, "Modeling and analysis of k-tier downlink heterogeneous cellular networks," *IEEE J. Sel. Topics Commun.*, vol. 30, no. 3, pp. 550–560, 2012.
- [16] N. Deng and M. Haenggi, "A fine-grained analysis of millimeter-wave device-to-device networks," *IEEE Trans. Commun.*, vol. 65, no. 11, pp. 4940–4954, 2017.
- [17] A. Al-Hourani, R. J. Evans, S. Kandeepan, B. Moran, and H. Eltom, "Stochastic geometry methods for modeling automotive radar interference," *IEEE Trans. Intell. Transp. Syst.*, vol. 19, no. 2, pp. 333–344, 2018.
- [18] A. Munari, L. Simić, and M. Petrova, "Stochastic geometry interference analysis of radar network performance," *IEEE Commun. Lett.*, vol. 22, no. 11, pp. 2362–2365, 2018.
- [19] G. Ghatak, S. S. Kalamkar, and Y. Gupta, "Radar detection in vehicular networks: Fine-grained analysis and optimal channel access," *IEEE Trans. Veh. Technol.*, vol. 71, no. 6, pp. 6671–6681, 2022.
- [20] P. Ren, A. Munari, and M. Petrova, "Performance analysis of a time-sharing joint radar-communications network," in *Int. Conf. Computing, Networking Commun. (ICNC)*, 2020, pp. 908–913.
- [21] J. Park and R. W. Heath, "Analysis of blockage sensing by radars in random cellular networks," *IEEE Signal Process. Lett.*, vol. 25, no. 11, pp. 1620–1624, 2018.
- [22] S. S. Ram, G. Singh, and G. Ghatak, "Optimization of radar parameters for maximum detection probability under generalized discrete clutter conditions using stochastic geometry," *IEEE Open J. Signal Process.*, vol. 2, pp. 571–585, 2021.
- [23] Y. Nabil, H. ElSawy, S. Al-Dharrab, H. Attia, and H. Mostafa, "A stochastic geometry analysis for joint radar communication system in millimeter-wave band," in *IEEE Int. Conf. Commun.*, 2023, pp. 5849–5854.
- [24] X. Gan, C. Huang, Z. Yang, X. Chen, J. He, Z. Zhang, C. Yuen, Y. Liang Guan, and M. Debbah, "Coverage and rate analysis for integrated sensing and communication networks," *IEEE J. Sel. Areas Commun.*, vol. 42, no. 9, pp. 2213–2227, 2024.
- [25] A. Salem, K. Meng, C. Masouros, F. Liu, and D. Lopez-Perez, "Rethinking dense cells for integrated sensing and communications: A stochastic geometric view," *IEEE Open J. Commun. Society*, vol. 5, pp. 2226–2239, 2024.
- [26] K. Meng, C. Masouros, G. Chen, and F. Liu, "Network-level integrated sensing and communication: Interference management and bs coordination using stochastic geometry," *arXiv preprint arXiv: 2311.09052*, 2023.
- [27] M. Haenggi, "Meta distributions—Part 1: Definition and examples," *IEEE Commun. Lett.*, vol. 25, no. 7, pp. 2089–2093, Jul. 2021.
- [28] M. Haenggi, "Meta distributions—Part 2: Properties and interpretations," *IEEE Commun. Lett.*, vol. 25, no. 7, pp. 2094–2098, Jul. 2021.
- [29] S. S. Ram, S. Singhal, and G. Ghatak, "Optimization of network throughput of joint radar communication system using stochastic geometry," *Frontiers Signal Process.*, vol. 2, p. 835743, 2022.
- [30] T. Bai, R. Vaze, and R. W. Heath, "Analysis of blockage effects on urban cellular networks," *IEEE Trans. Wireless Commun.*, vol. 13, no. 9, pp. 5070–5083, 2014.
- [31] A. Thornburg, T. Bai, and R. W. Heath, "Performance analysis of outdoor mmwave ad hoc networks," *IEEE Trans. Signal Process.*, vol. 64, no. 15, pp. 4065–4079, 2016.
- [32] T. Wild, V. Braun, and H. Viswanathan, "Joint design of communication and sensing for beyond 5G and 6G systems," *IEEE Access*, vol. 9, pp. 30 845–30 857, 2021.
- [33] A. Baddeley, P. Gregori, J. Mateu, R. Stoica, and D. Stoyan, *Case Studies in Spatial Point Process Modeling. Lecture Notes in Statistics*. Springer, 2006.
- [34] M. A. Richards, *Fundamentals of radar signal processing*. Mcgraw-hill New York, 2005, vol. 1.
- [35] D. Shnidman, "Expanded swerling target models," *IEEE Trans. Aerosp. Electron. Syst.*, vol. 39, no. 3, pp. 1059–1069, 2003.
- [36] T. Bai and R. W. Heath, "Coverage and rate analysis for millimeter-wave cellular networks," *IEEE Trans. Wireless Commun.*, vol. 14, no. 2, pp. 1100–1114, 2014.
- [37] J. Gil-Pelaez, "Note on the inversion theorem," *Biometrika*, vol. 38, no. 3-4, pp. 481–482, Dec. 1951.
- [38] W. Cheng, Z. Zhao, H. H. Yang, W. Hong, T. Q. Quek, and Z. Ding, "On the study of success serving probability for integrated sensing and communication (ISAC) based on stochastic geometry," in *IEEE Int. Conf. Commun*, 2024, pp. 5098–5103.
- [39] W. Yi, Y. Liu, Y. Deng, and A. Nallanathan, "Clustered uav networks with millimeter wave communications: A stochastic geometry view," *IEEE Trans. Commun.*, vol. 68, no. 7, pp. 4342–4357, 2020.
- [40] C. Balanis, *Antenna Theory: Analysis and Design*. Wiley, 2015. [Online]. Available: <https://books.google.com/books?id=u-xbCwAAQBAJ>
- [41] H. H. Yang, T. Q. S. Quek, and H. V. Poor, "A unified framework for SINR analysis in Poisson networks with traffic dynamics," *IEEE Trans. Commun.*, vol. 69, no. 1, pp. 326–339, Jan. 2021.
- [42] H. H. Yang, C. Xu, X. Wang, D. Feng, and T. Q. S. Quek, "Understanding age of information in large-scale wireless networks," *IEEE Trans. Wireless Commun.*, vol. 20, no. 5, pp. 3196–3210, May 2021.